INTERNATIONAL JOURNAL FOR NUMERICAL METHODS IN FLUIDS, VOL. 6, 365–386 (1986)

FINITE ELEMENT METHOD FOR MOVING BOUNDARY PROBLEMS IN RIVER FLOW

MUTSUTO KAWAHARA

Department of Civil Engineering, Chuo University, Kasuga, Bunkyo-ku, Tokyo, 112, Japan

AND

TSUYOSHI UMETSU

Department of Civil Engineering, Chuo University, Kasuga, Bunkyo-ku, Tokyo, 112, Japan

INTRODUCTION

To analyse river flow and to clarify velocity and water elevation are highly important and valuable in the field of engineering for the purposes of the design of river structures, prediction of water quality, estimation of flood damage, etc. The governing equation of river flow can be described by the shallow water theory in which the effect of the gravity force due to the inclination of the river bed is considered. Usually, two types of the shallow water equations are used in these analyses, of which one employs velocity and water elevation as unknown variables and the other uses discharge and water elevation. In this paper, the latter formulation is used for computational convenience. For instance, as the boundary condition at the upstream site, the discharge condition is more convenient because discharge, not velocity, is usually observed in field measurements.

A few finite element methods have been presented previously for the analysis of river flow. Cochet *et al.*[1] investigated the finite element method of steady river flow using the penalty method. Su and Wang[2] examined the quadratic finite element with a third-order time discretization scheme. Lee[3] presented the method for the analysis of flood plains. Research by Baker and Soliman[4] is concerned with river flow analysis.

This paper presents the two-step explicit finite element method,[5–10] which has been successfully applied to solve the shallow water equation of river flow. The linear interpolation functions for both discharge and water elevation have been used based on the three node triangular finite element. In the analysis of this paper, the treatment of the boundary configuration, which moves according to whether the water elevation increases or decreases, is considered. The principal author presented a method to deal with the movement of the boundary in a previous paper.[5] However, stable computations sometimes could not be obtained using the previous method. Thus, the method has been improved to ensure numerical stability.

Distinctive features of the analysis in this paper are summarized as follows. First, the finite element method is presented taking into account the effect of the gravity force. The selective lumping two-step explicit method is shown to be effective in the analysis. Secondly, the treatment of the moving boundary is presented using the improved algorithm based on the previously presented method. Thirdly and finally, three examples, i.e. flow through a channel with a rigid wall, flow through a channel with exposed mounds at the channel bed and the actual Arakawa

0271–2091/86/060365–22$11.00

Received 1 March 1985
Revised 22 January 1986

River, are computed numerically. These features show that the finite element method presented in this paper is a useful tool for the analysis of river flow.

BASIC EQUATIONS

The behaviour of river flow can be regularly expressed by the shallow water equation. The Cartesian co-ordinate is placed at the still water level on the surface of the river as shown in Figure 1. Equations in this paper are written employing the indicial notation and the summation convention with repeated indices. The horizontal co-ordinates are expressed by $x_i (i = 1, 2)$ and time is t. Differentiations with respect to x_i and t are denoted by subscripted comma and superscripted dot, respectively. It is reasonable to assume hydrostatic pressure distribution in the water depth direction, considering that the horizontal length scales are far larger than the water depth scale. The equations of motion and continuity can be described in the following form:

$$\dot{M}_i + (U_j M_i)_{,j} + \frac{g}{2}\cos\theta\cos\varphi(H+\eta)^2_{,i} - A_1(M_{i,j} + M_{j,i})_{,j} + f M_i\sqrt{(M_k M_k)} = g(H+\eta)\Theta_i, \quad (1)$$

$$\dot{\eta} + M_{i,i} = 0, \quad (2)$$

where U_i and η denote mean velocity and water elevation, M_i is discharge per unit width, i.e.

$$M_i = U_i(H+\eta) \quad (3)$$

and H, A_1, g and f represent water depth, turbulent viscosity, gravity acceleration and friction coefficient, respectively. The gravity contribution is expressed by Θ_i, i.e.

$$\Theta_1 = \sin\theta, \quad (4)$$

$$\Theta_2 = \sin\varphi, \quad (5)$$

where the mean gradients of the river bottom for both x and y directions are written as θ and ϕ, respectively. Thus, equation (1) includes the effect of gravity due to the inclination of the river bottom.

As the boundary conditions, the following three types are considered. On the boundary S_1, the discharge is postulated in the form

$$M_i = \hat{M}_i, \qquad \text{on} \quad S_i, \quad (6)$$

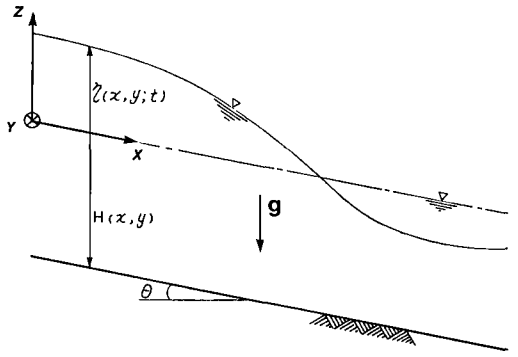

Figure 1. Co-ordinate system

where superscripted ˆ means the value which is prescribed on the boundary. The vertically integrated surface flux r_i is given on the boundary S_2 by

$$r_i = \{A_1(M_{i,j} + M_{j,i})\} n_j = \hat{r}_i, \quad \text{on} \quad S_2, \tag{7}$$

where δ_{ij} denotes the Kronecker delta and n_j is the unit normal to the boundary. The water elevation is given on the boundary S_3,

$$\eta = \hat{\eta}, \qquad \text{on} \quad S_3. \tag{8}$$

The whole boundary S of the flow field V to be analysed consists of S_1 and S_2 only, and S_1 and S_2 do not overlap. The boundary S_3 is a part of S_2. The basic equations treated in this paper are equations (1)–(5) with boundary conditions (6)–(8).

FINITE ELEMENT EQUATIONS

The shallow water equation has been formulated based on the vertically integrated form taking water discharge and elevation as field variables. In the practical analysis, a great number of nodal points and elements are required to express the precise behaviour of river flow in detail. Therefore, to save the computer core storage and computational time, the two-step explicit method is usefully employed, of which the precise formulation has been presented elsewhere.

The flow field to be analysed is divided into triangular finte elements, for which discharge M_i and water elevation η are interpolated as

$$M_i = \Phi_\alpha M_{\alpha i}, \tag{9}$$

$$\eta = \Phi_\alpha \eta_\alpha, \tag{10}$$

where Φ_α denotes a linear interpolation function, $M_{\alpha i}$ denotes nodal values of discharge at the αth node of an element in the ith direction and η_α are nodal values of water elevation at the αth node.

The total time interval to be analysed is also divided into time increments, of which the interval is denoted by Δt. A superscripted n indicates nodal values at the nth time point. The final equation of the two-step explicit finite element method can be expressed in the following form:

for the first step:

$$\begin{aligned}\bar{A}_{\alpha\beta} M^{n+1/2}_{\beta i} = \bar{A}_{\alpha\beta} M^{n}_{\beta i} - \frac{\Delta t}{2}[&B_{\alpha\beta j\gamma} U^{n}_{\beta j} M^{n}_{\gamma i} + C_{\alpha\beta\gamma j} U^{n}_{\beta j} M^{n}_{\gamma i} + S_{\alpha i\beta j} M^{n}_{\beta j} \\ &+ F_{\alpha\beta\gamma i}(H_\beta + \eta^n_\beta)(H_\gamma + \eta^n_\gamma) - A_{\alpha\beta}(H_\beta + \eta^n_\beta) g\Theta_i + \bar{A}_{\alpha\beta}\lambda M^n_{\beta i} - \Omega_{\alpha i}],\end{aligned} \tag{11}$$

$$\bar{A}_{\alpha\beta}\eta^{n+1/2}_\beta = \tilde{A}_{\alpha\beta}\eta^n_\beta - \frac{\Delta t}{2} G_{\alpha\beta i} M^n_{\beta i}, \tag{12}$$

and for the second step:

$$\begin{aligned}\bar{A}_{\alpha\beta} M^{n+1}_{\beta i} = \bar{A}_{\alpha\beta} M^{n}_{\beta i} - \Delta t[&B_{\alpha\beta j\gamma} U^{n+1/2}_{\beta j} M^{n+1/2}_{\gamma i} + C_{\alpha\beta\gamma j} U^{n+1/2}_{\beta j} M^{n+1/2}_{\gamma i} \\ &+ S_{\alpha i\beta j} M^{n+1/2}_{\beta j} + F_{\alpha\beta\gamma i}(H_\beta + \eta^{n+1/2}_\beta)(H_\gamma + \eta^{n+1/2}_\gamma) \\ &- A_{\alpha\beta}(H_\beta + \eta^{n+1/2}_\beta) g\Theta_i + \bar{A}_{\alpha\beta}\lambda M^{n+1/2}_{\beta i} - \Omega_{\alpha i}],\end{aligned} \tag{13}$$

$$\bar{A}_{\alpha\beta}\eta^{n+1}_\beta = \tilde{A}_{\alpha\beta}\eta^n_\beta - \Delta t\, G_{\alpha\beta i} M^{n+1/2}_{\beta i}, \tag{14}$$

where

$$A_{\alpha\beta} = \int_V (\Phi_\alpha \Phi_\beta) \mathrm{d}V, \quad B_{\alpha\beta j\gamma} = \int_V (\Phi_\alpha \Phi_{\beta,j} \Phi_\gamma) \mathrm{d}V, \quad C_{\alpha\beta\gamma j} = \int_V (\Phi_\alpha \Phi_\beta \Phi_{\gamma,j}) \mathrm{d}V,$$

$$S_{\alpha i\beta j} = \int_V A_1 (\Phi_{\alpha,k} \Phi_{\beta,k}) \delta_{ij} \mathrm{d}V + \int_V A_1 (\Phi_{\alpha,j} \Phi_{\beta,i}) \mathrm{d}V,$$

$$F_{\alpha\beta\gamma j} = \int_V g \cos\theta \cos\varphi (\Phi_\alpha \Phi_\beta \Phi_{\gamma,i}) \mathrm{d}V, \quad G_{\alpha\beta i} = \int_V (\Phi_\alpha \Phi_{\beta,i}) \mathrm{d}V,$$

$$\lambda = f\sqrt{(M_{\alpha k} M_{\alpha k})}, \quad \Omega_{\alpha i} = \int_{S_2} (\Phi_\alpha \hat{r}_i) \mathrm{d}S,$$

in which V is the area of a finite element of which the boundary is S. In equations (11)–(14), $\bar{A}_{\alpha\beta}$ means the lumped coefficient of $A_{\alpha\beta}$, and $\tilde{A}_{\alpha\beta}$ is the mixed coefficient which is

$$\tilde{A}_{\alpha\beta} = e\bar{A}_{\alpha\beta} + (1 - e)A_{\alpha\beta}, \tag{15}$$

where e is referred to as the lumping parameter. The conventional superposition procedure leads to the finite element equation of the global form. The nodal velocity $U_{\beta i}$ can be computed from the nodal discharge $M_{\beta i}$ divided by the water elevation η_β.

TREATMENT OF MOVING BOUNDARY

It is valuable and almost indispensable to introduce how to compute the movement of the boundary configuration in the analysis of river flow. That means how to decide which part of the river bottom is exposed. In this paper, the computation has been carried out depending on the following criteria:

At first, it must be decided if the river bottom is covered with water or not, which can be deduced from the following equations: if $h = -H + \eta < 0$ then the bottom is exposed, and if $h = -H + \eta > 0$ then the bottom is submerged, where H and η express water depth and water elevation, respectively; both are computed from the mean water level.

Secondly, one can decide if a finite element is exposed or submerged. If two of the three nodal values of h at a finite element are greater than zero, the element is omitted from the computation.

Thirdly, one must decide which element is located on the boundary between land and river. If one nodal value of h of an element is greater than zero, the element is decided to be on the boundary. In this case, two components of discharge at three nodal points of the finite element are specified to be zero. One water elevation, which is computed as $h < 0$, is also specified to be zero, whereas the other two nodal values of water elevation are included in the computation.

Finally, the next iteration cycle is repeated using the new specified boundary conditions based on the revised finite element idealization. This revision is carried out at both the first and second time steps of the two-step scheme.

Figure 2 illustrates the above explained treatment of the moving boundary. Finite elements are numbered as ①, ②, ③, ④,... and nodal points are 1, 2, 3, 4,.... Then, for example, the following treatment is performed:

1. Element ① with nodes 1, 2 and 11, and element ② with nodes 11, 10 and 1 are omitted from the computation because all their water elevations are greater than zero.
2. Element ③ with nodes 2, 3 and 12, and element ④ with nodes 12, 11 and 2 are used in the

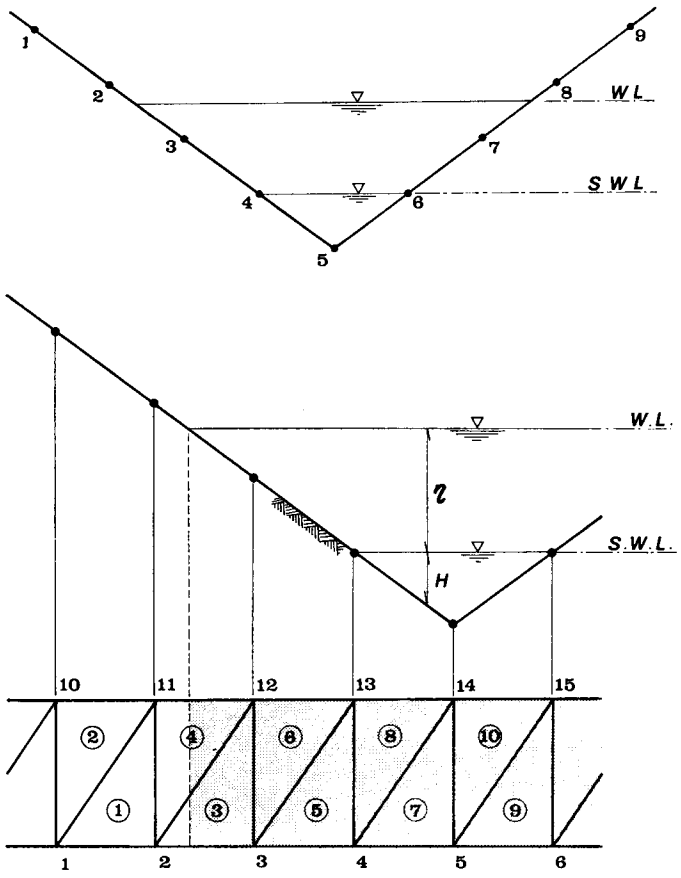

Figure 2. Schematic illustration of moving boundary

computation, specifying both discharge components at nodes 2, 3, 11 and 12 and the water elevation at nodes 2 and 11 to be all zero.

3. Element ⑤ with nodes 3, 4 and 13 and element ⑥ with nodes 13, 12 and 3 are included in the computation.

According to the authors' numerical experiments, stable computations have been obtained based on the computational technique presented in this paper. But, it may be noticeable that the speed of movement the boundary in this computation would be slower than in the actual movement.

NUMERICAL EXAMPLE

As the first computation, flow through an open channel with a solid wall is computed. Figure 3 shows the plan view with the finite element idealization and the vertical view of the channel employed in the computation. Section A–B is entrance of the channel. At section C–L, the width is suddenly expanded. At sections J–E and I–F, the bottom inclination is changed. Section H–G is the outlet. The length of the channel is 180 m, and the widths of entrance and outlet are 8 m and 20 m, respectively. The total numbers of nodal points and finite elements are 3427 and 6456,

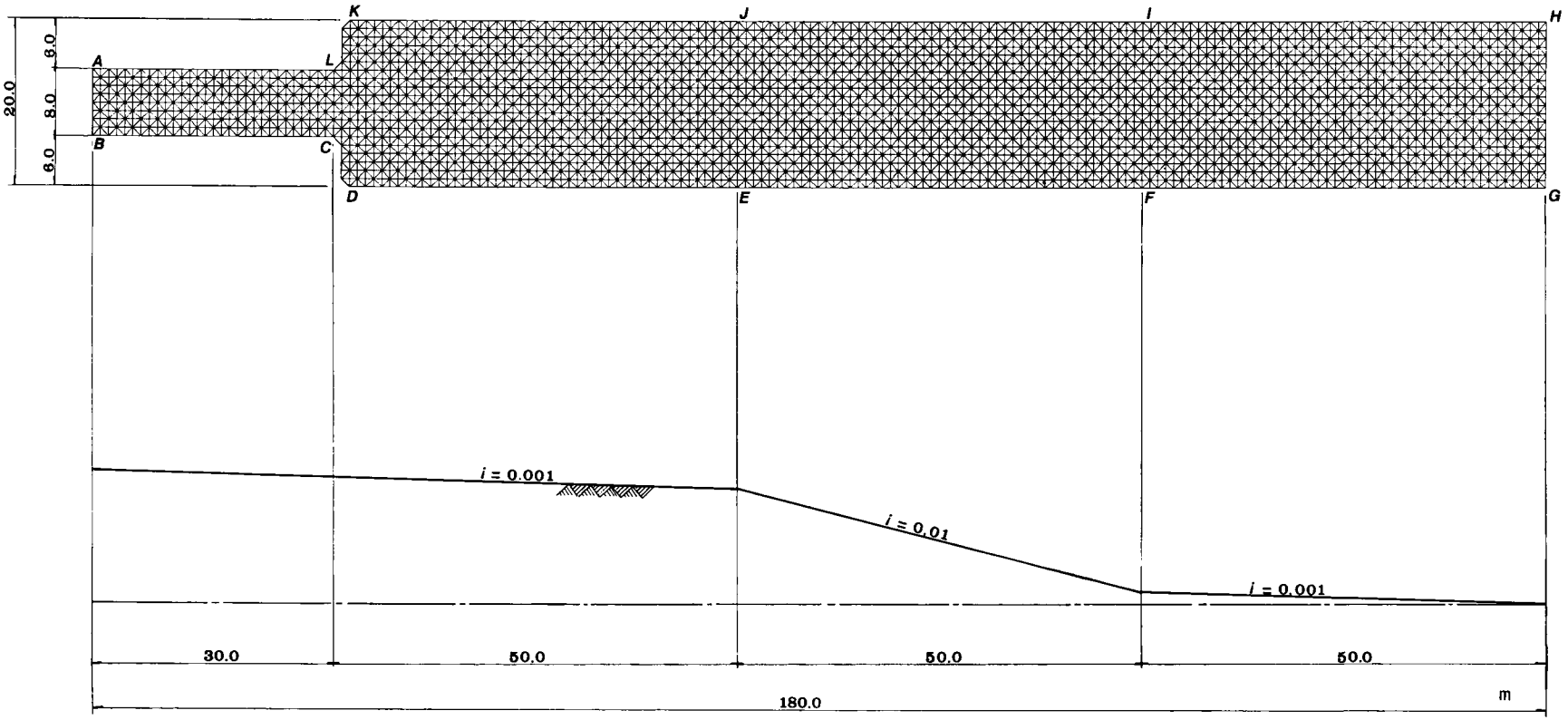

Figure 3. Finite element idealization of open channel

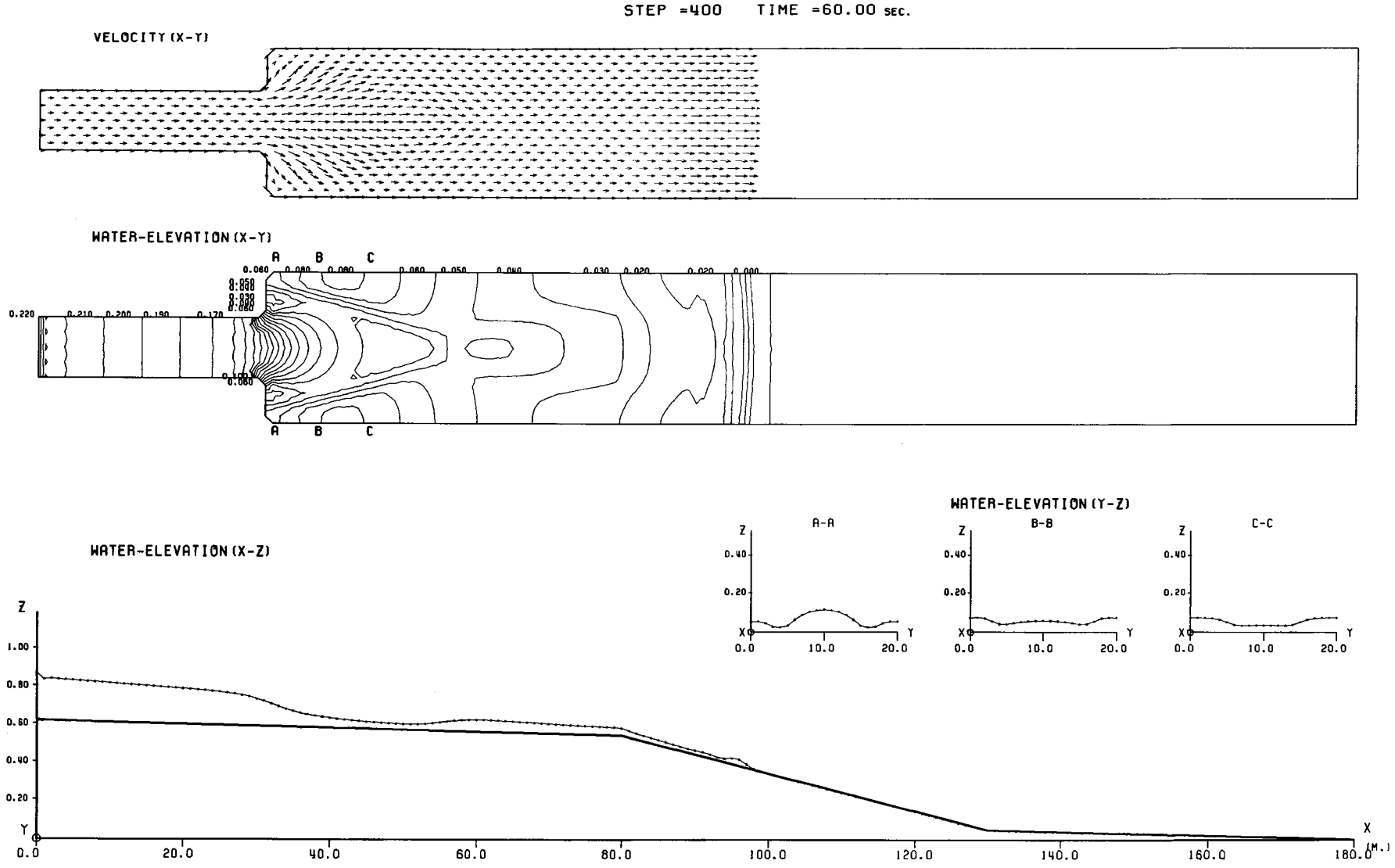

Figure 4. Compound results at 60 s

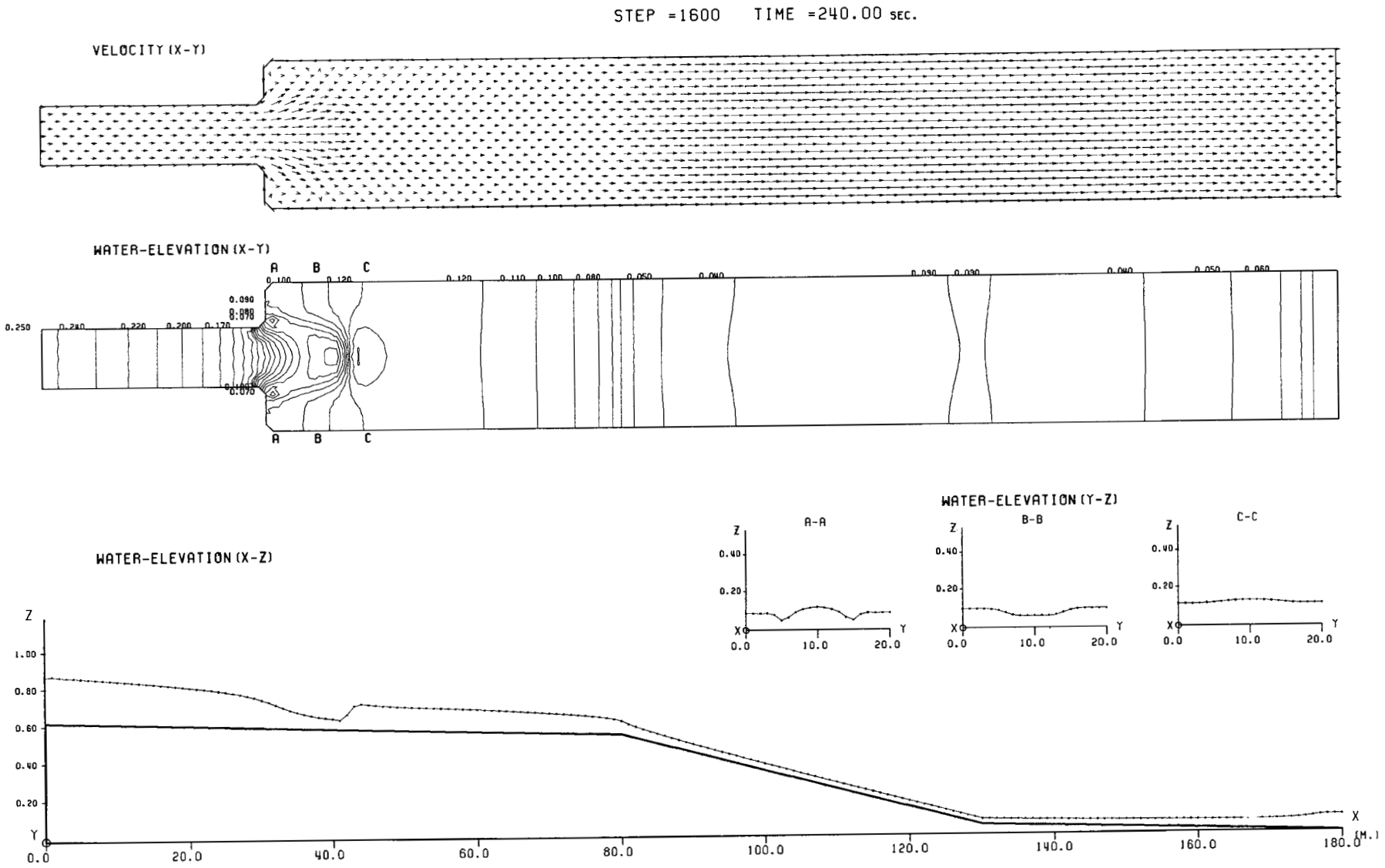

Figure 5. Computed results at 240 s

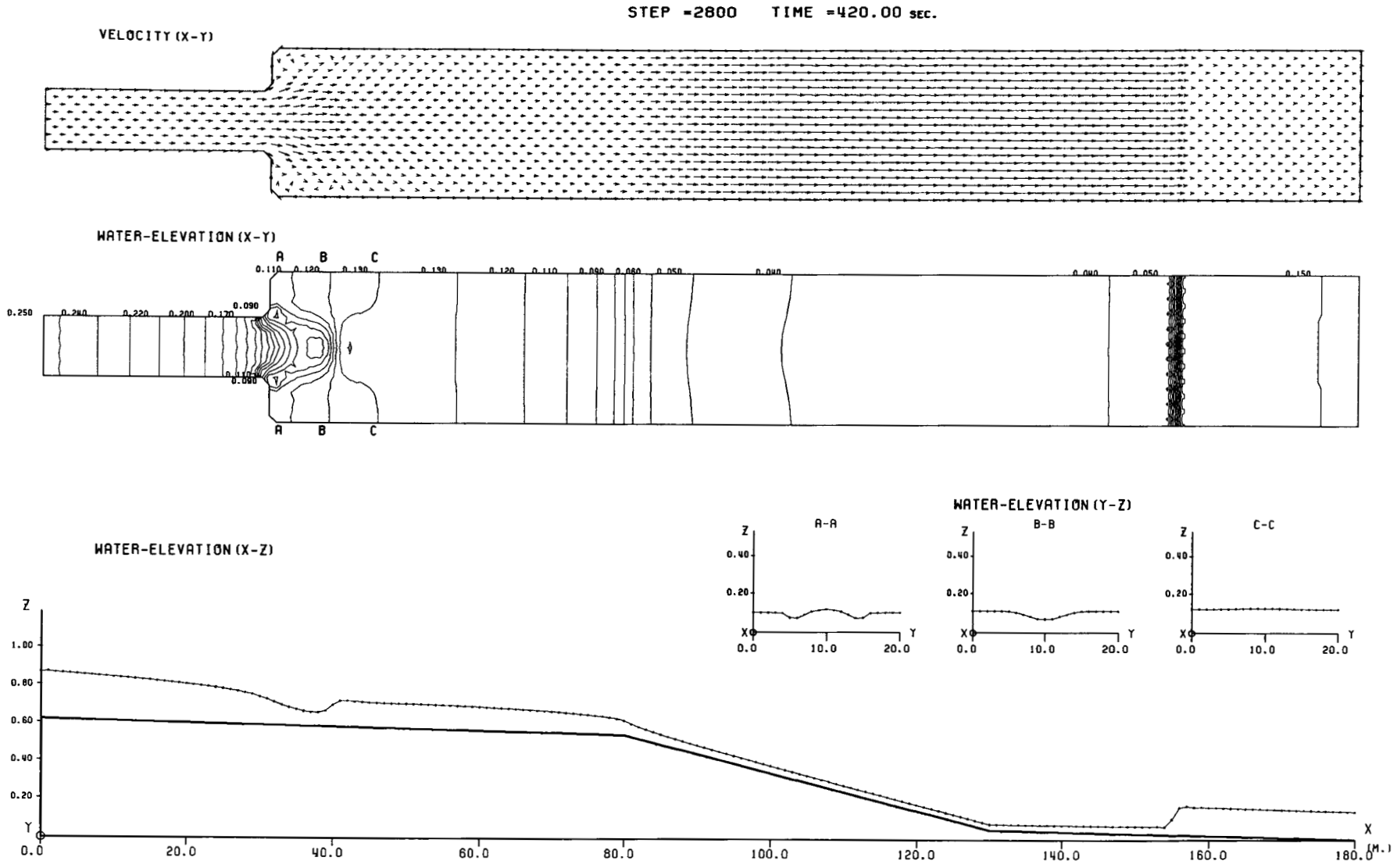

Figure 6. Computed results at 420 s

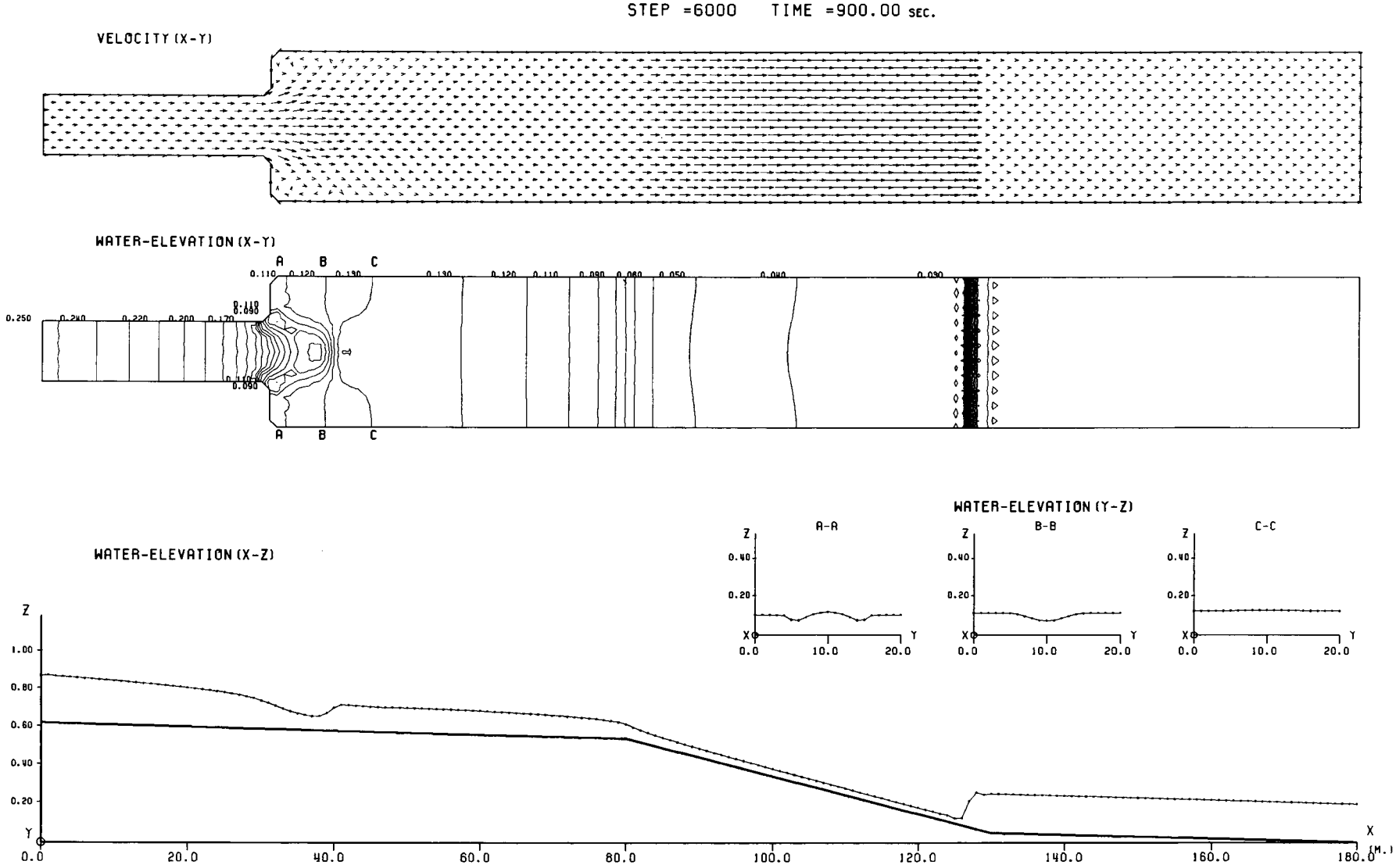

Figure 7. Computed results at 900 s

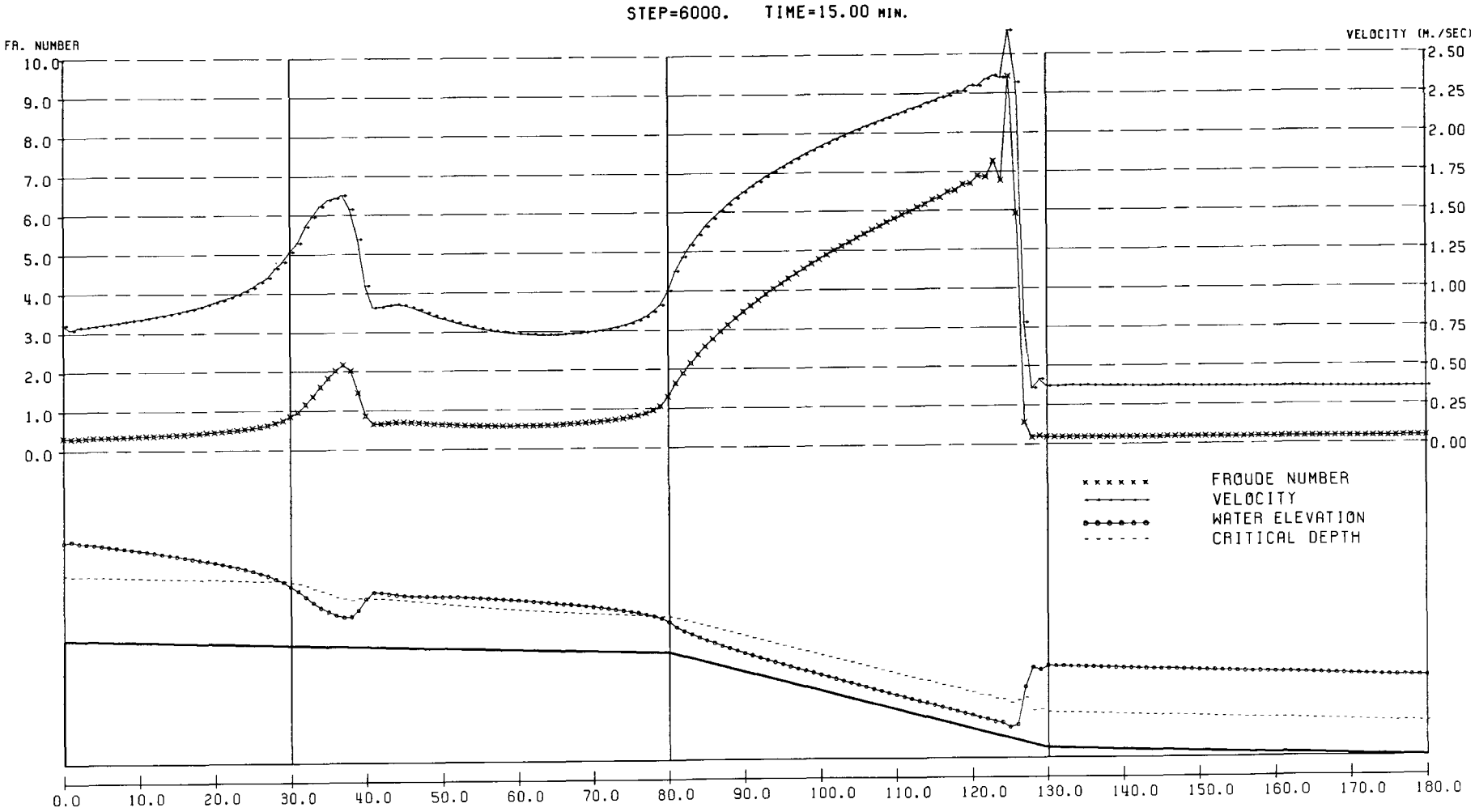

Figure 8. Illustrations of ordinary and jet flows

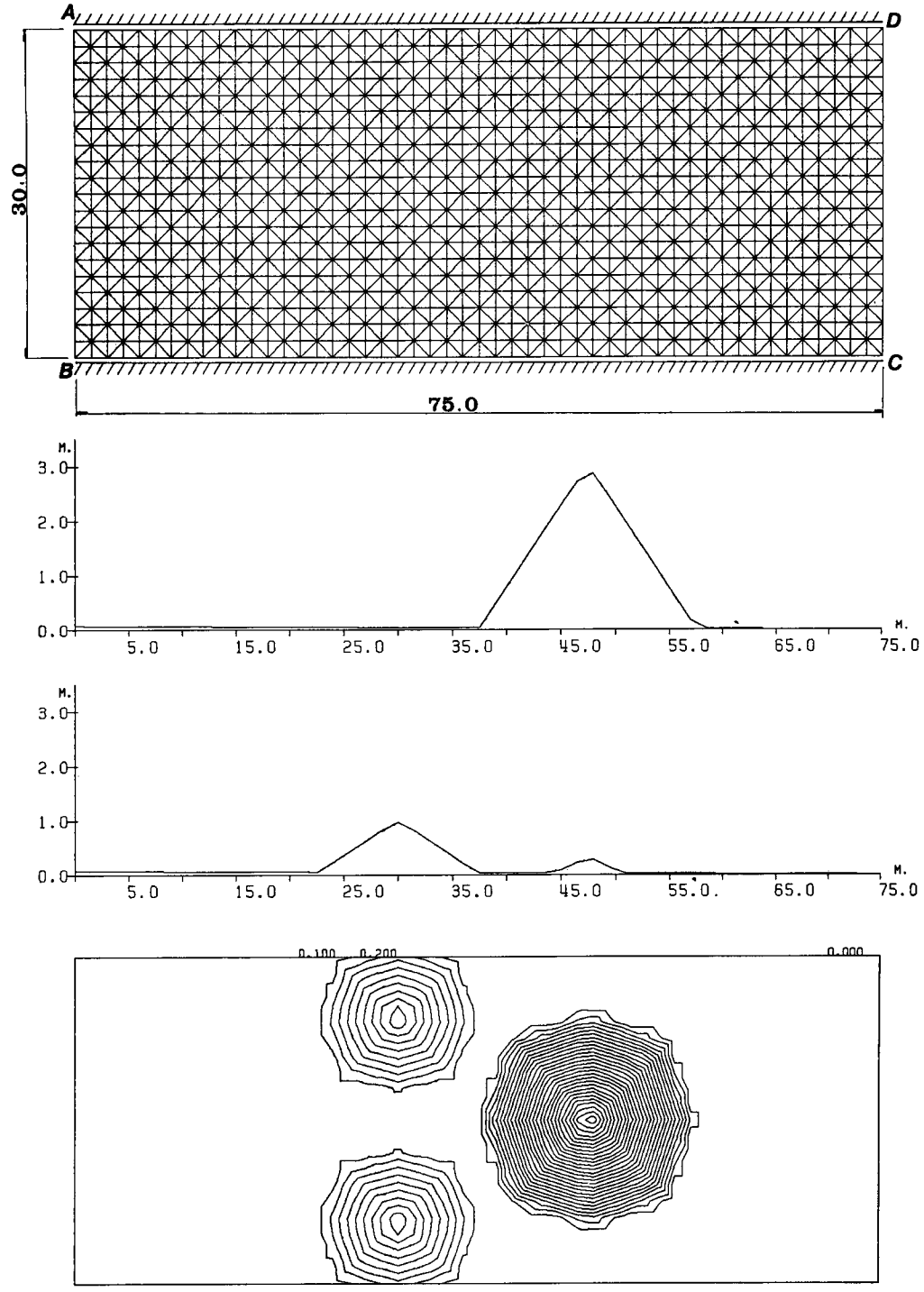

Figure 9. Finite element idealization of open channel with mound

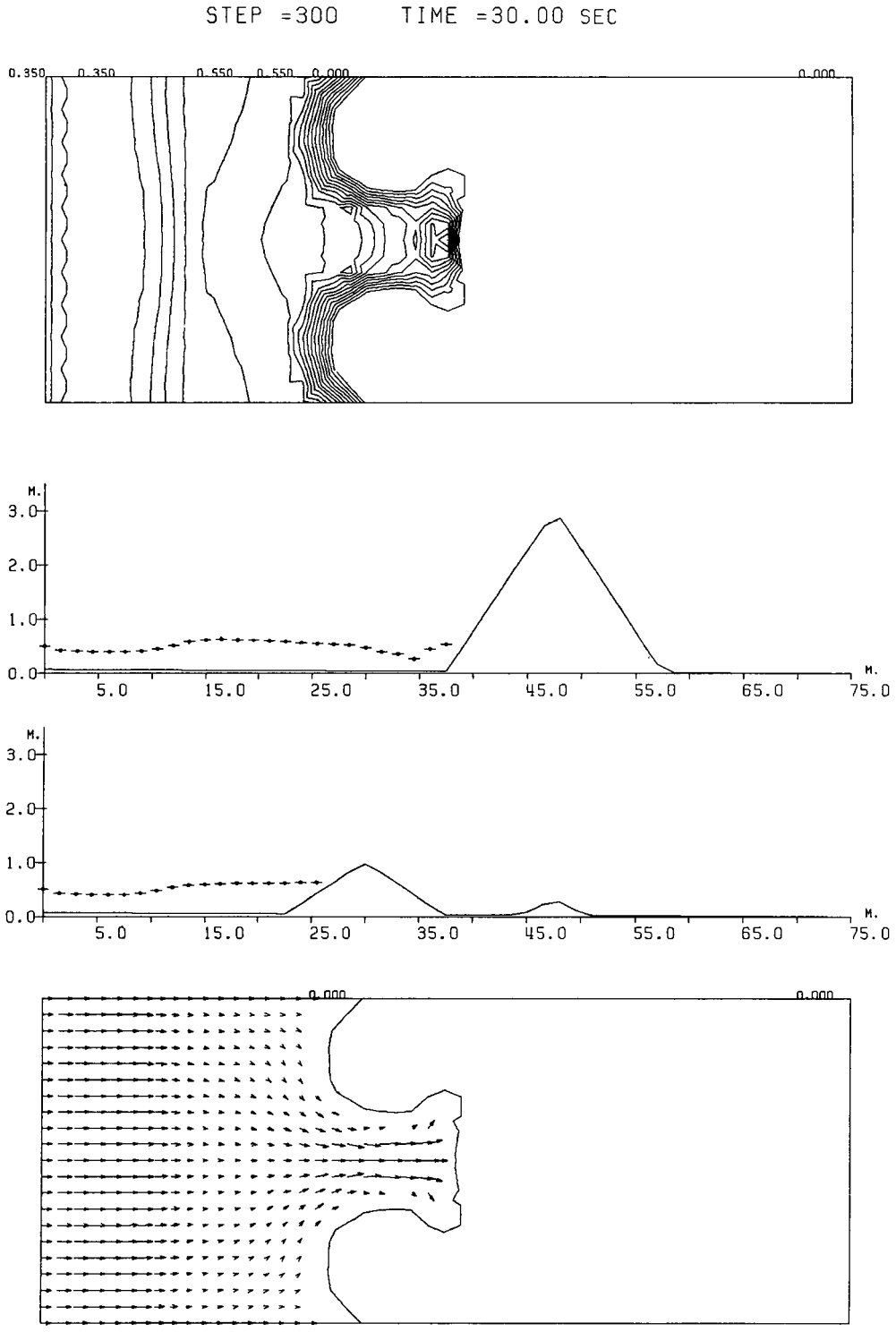

Figure 10. Computed results at 30 s

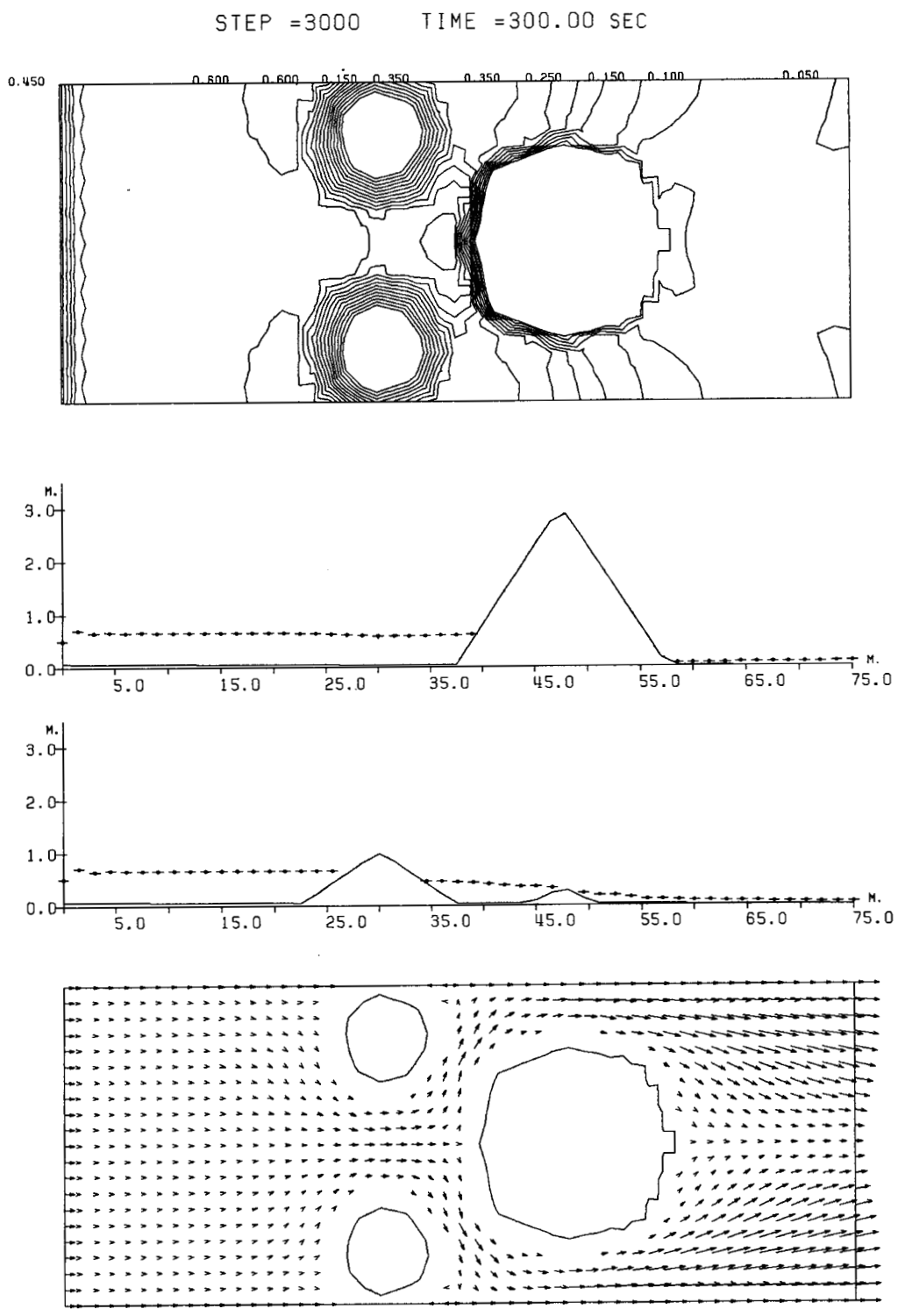

Figure 11. Computed results at 300 s

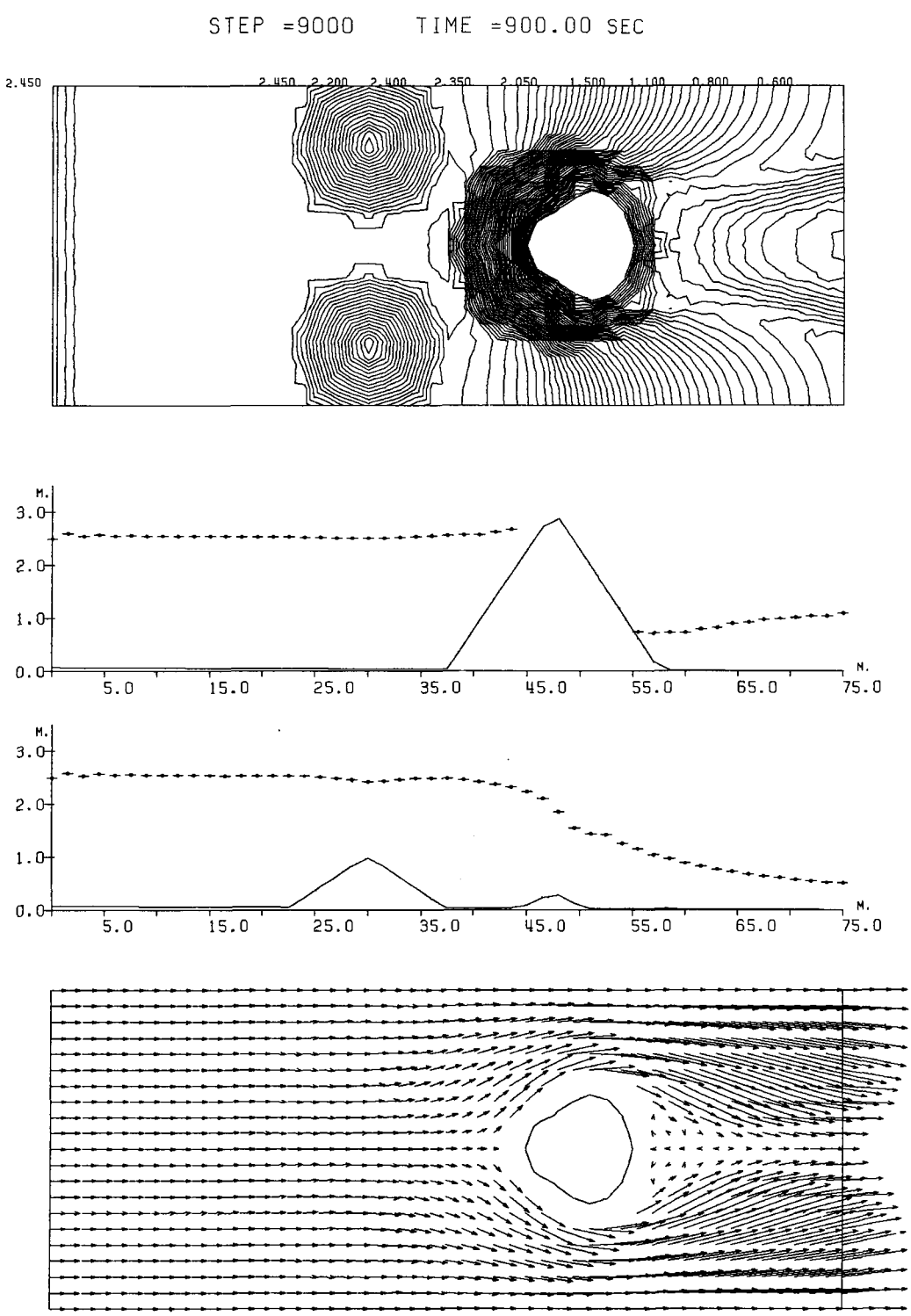

Figure 12. Computed results at 900 s

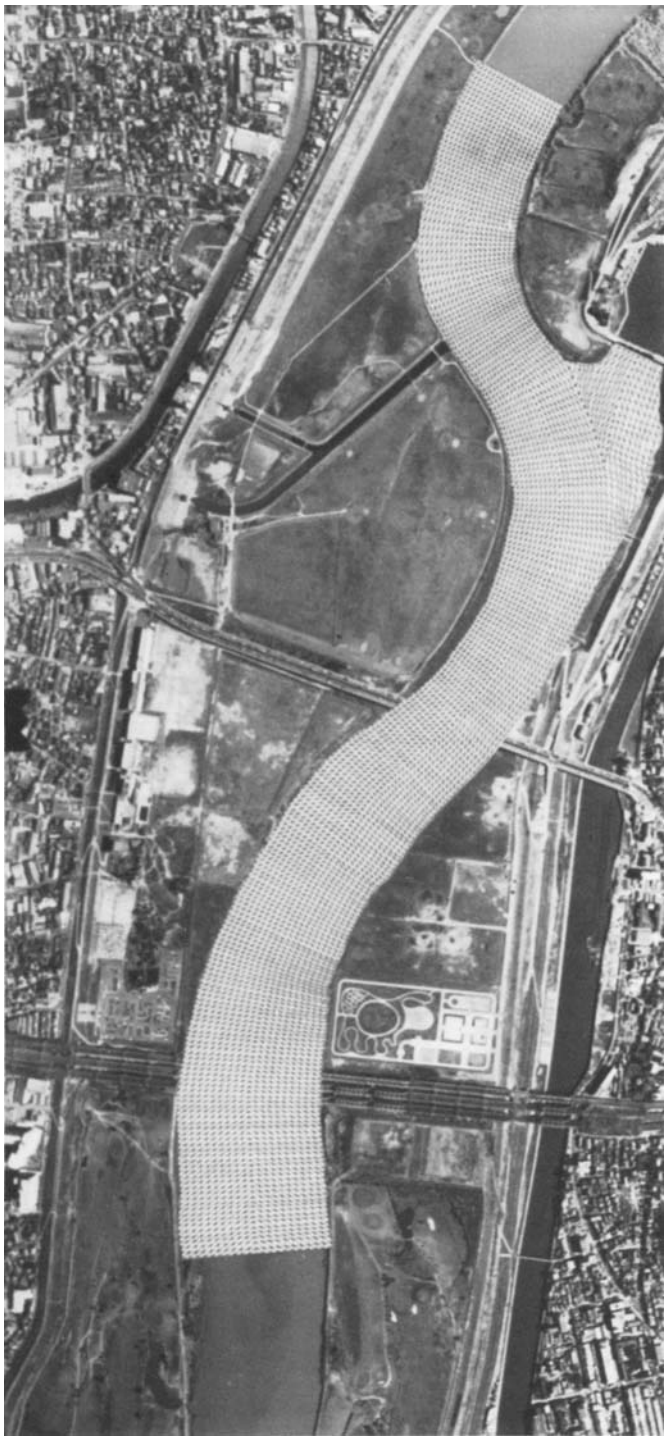

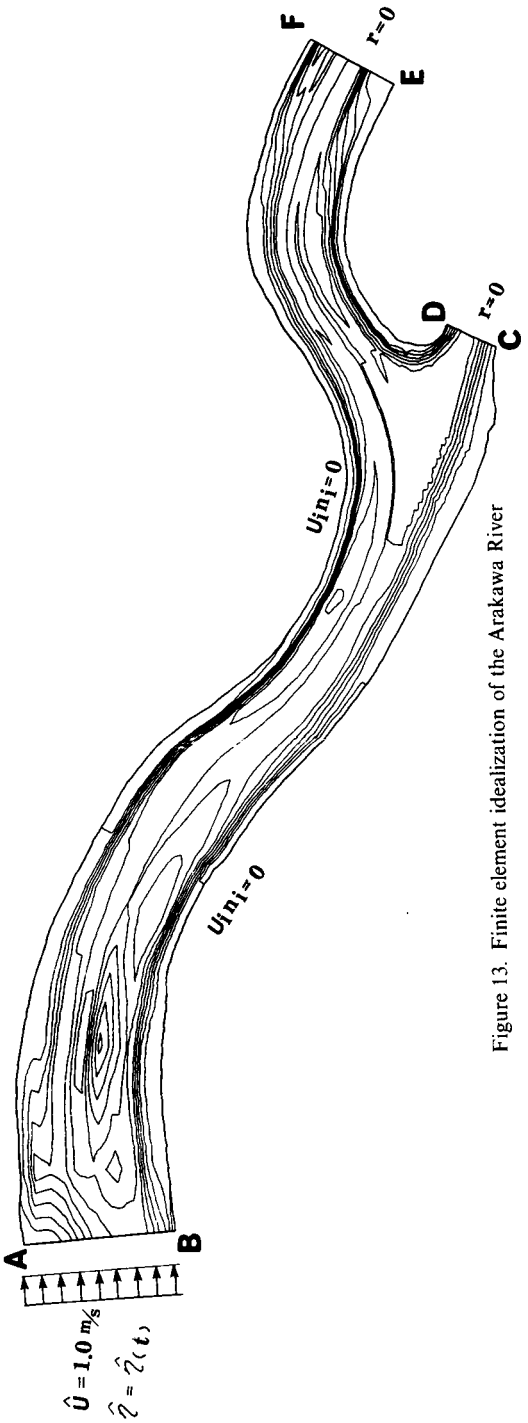

Figure 13. Finite element idealization of the Arakawa River

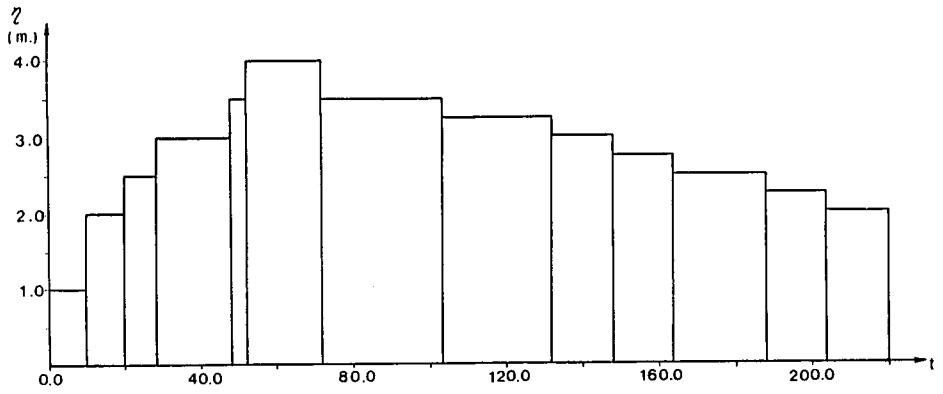

Figure 14. Variation of water elevation

respectively. Assuming that the longitudinal component of discharge M_n on the boundary A–B is imposed as $M_n = 0{\cdot}2\ \mathrm{m}^2/\mathrm{s}$, and that both components of velocity on the boundaries are specified to be zero, the computed velocity and water elevation are plotted in Figures 4–7. At steady state, the Froude number Fr and critical depth H_c are calculated and illustrated in Figure 8. The small arrow mark → means the computed velocity along the centre line of the channel. The Froude number, based on the computed velocity divided by the square root of the product of gravity acceleration and the computed water elevation, is denoted by the mark ⊗. The critical depth H_c is computed by

$$H_c = \sqrt[3]{\left(\frac{Q^2}{gB^2}\right)}, \tag{16}$$

where Q is the discharge and B is the width of the channel. The critical depth is plotted with the computed elevation. From the Figure, the flow regions corresponding to the ordinary flow and jet flow can be clearly seen. The hydraulic jump is also clearly computed.

As the second computation, flow through a channel with three mounds located on the channel bottom is computed to test procedures for the moving boundary. A finite element idealization and contour lines of the bottom topography are shown in Figure 9. The total numbers of nodal points and finite elements are 1071 and 2000, respectively. The length of the channel is 75 m and its width is 30 m. The contour lines are drawn for every 10 cm of height. On the boundary A–B, the longitudinal velocity $U_n = 1\ \mathrm{m/s}$ is always assigned and on the boundaries A–D and B–C, the velocity normal to the boundary is assumed to be zero. Water elevation on the boundary A–B is specified as follows. From step 0 to step 3000 $\eta = 0{\cdot}5$ m. From step 3001 to step 3500 $\eta = 1{\cdot}0$ m. Namely, the water elevation is given as $\eta = 0{\cdot}5$ m on the boundary A–B and, confirming that the flow has reached the steady state, which is satisfactory at step 3000 and later, the water elevation is raised up to $\eta = 1{\cdot}0$ m. The eddy viscosity $A_1 = 0{\cdot}4\ \mathrm{m}^2/\mathrm{s}$ and the friction coefficient $\lambda = 0{\cdot}008\ \mathrm{s}^{-1}$ are used. For the time increment, $\Delta t = 0{\cdot}10$ s is employed. Computed water elevation and velocity are illustrated in Figures 10–12 at steps 300, 3000 and 9000. It is seen in Figures 9 and 11 that the water front is moving downward to the down stream. In Figure 11 the steady state can be confirmed. It is clearly shown in Figure 12 that the two mounds at the bottom are completely submerged under the water.

As the final computation, the river flow of the Arakawa River is computed. A finite element idealization and bottom topography are shown in Figure 13. The total numbers of nodal points

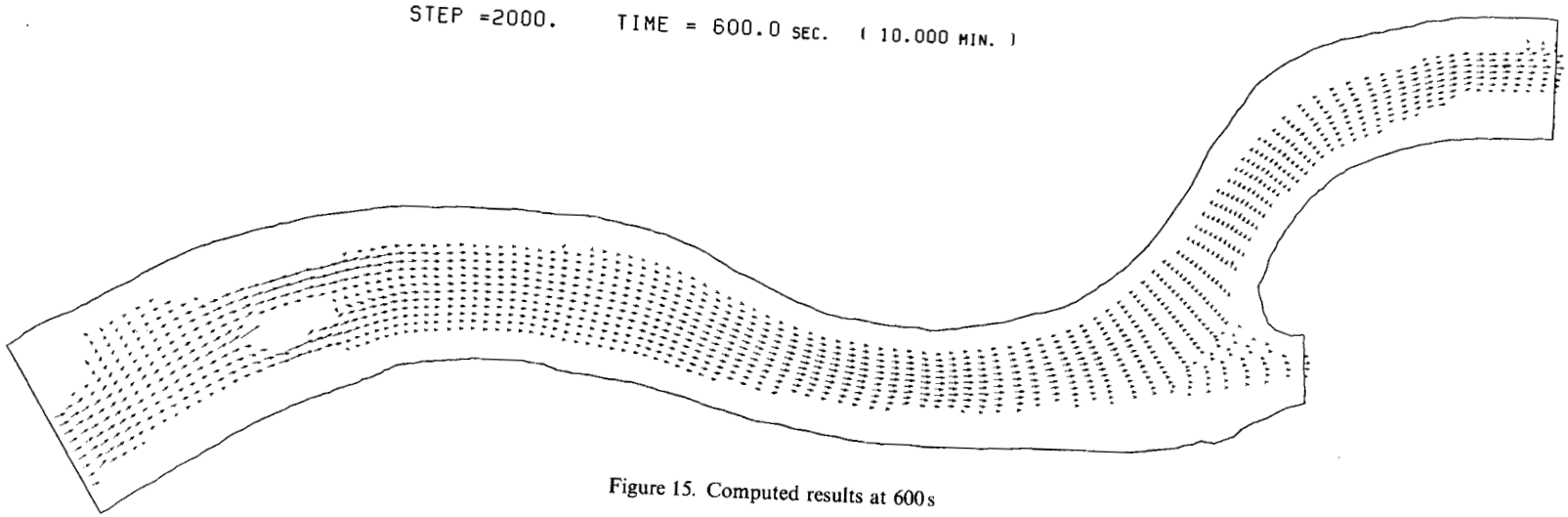

Figure 15. Computed results at 600 s

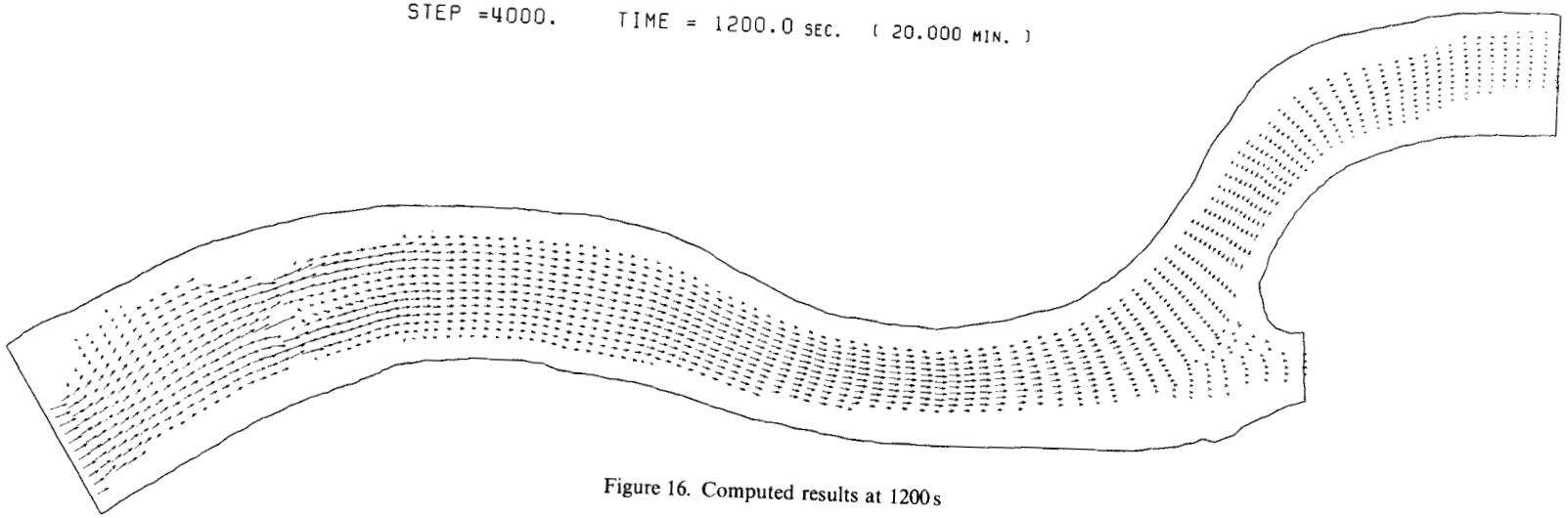

Figure 16. Computed results at 1200 s

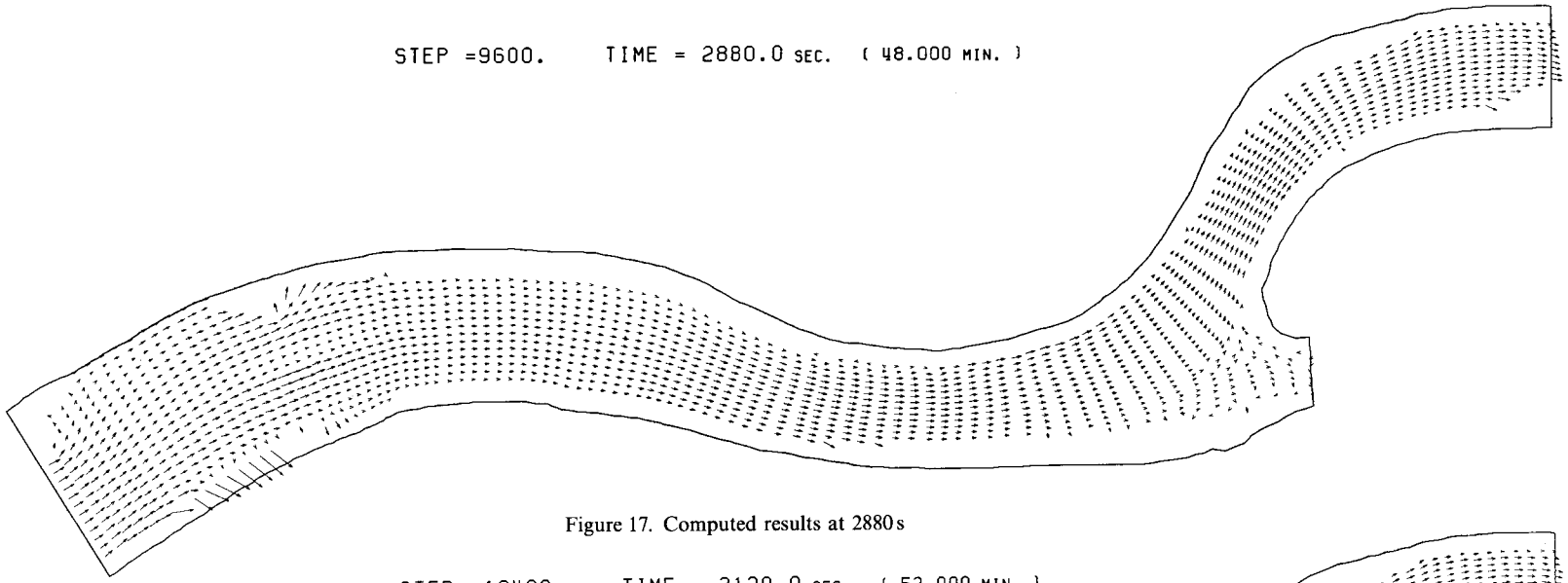

Figure 17. Computed results at 2880 s

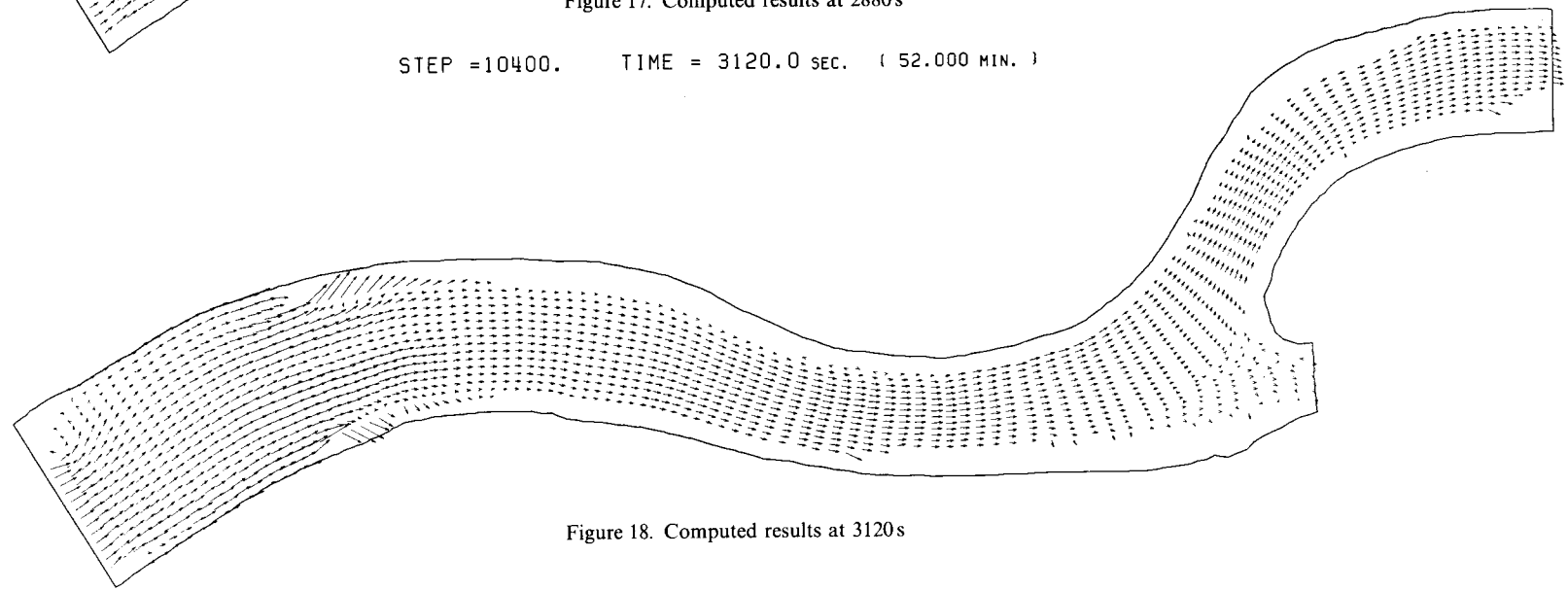

Figure 18. Computed results at 3120 s

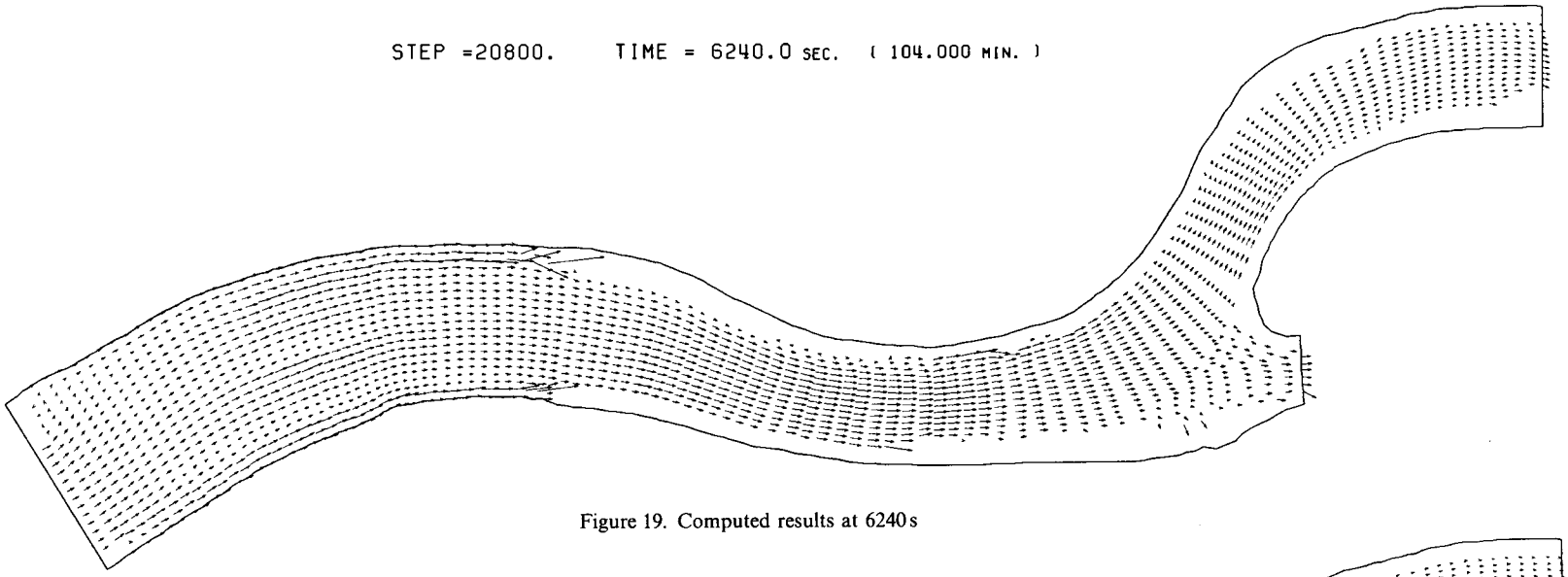

Figure 19. Computed results at 6240 s

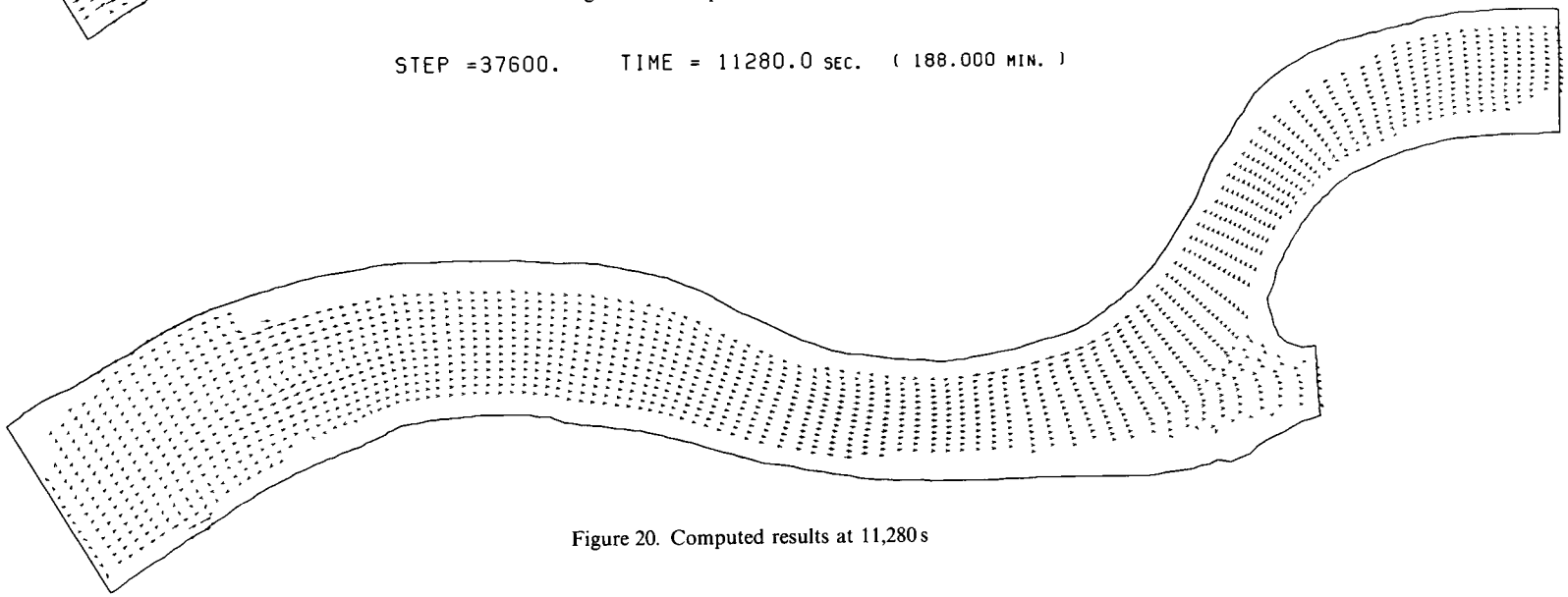

Figure 20. Computed results at 11,280 s

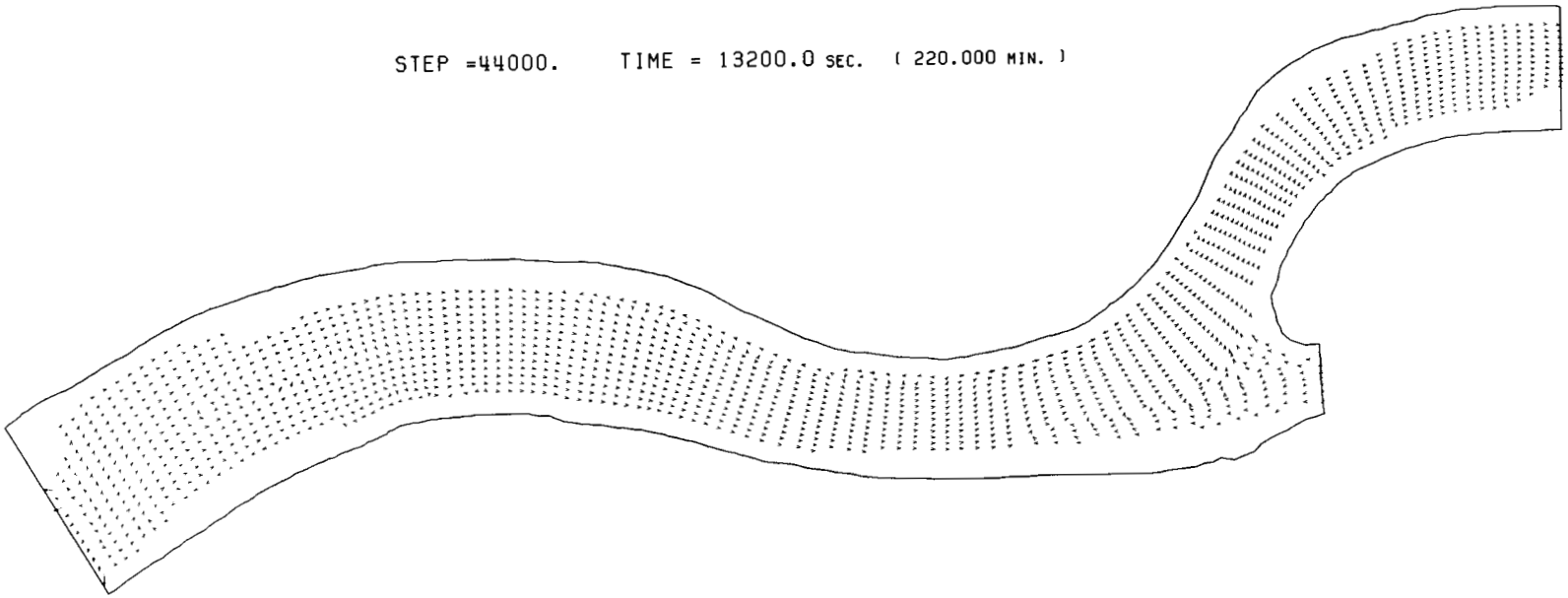

Figure 21. Computed results at 13,200 s

and finite elements are 5333 and 10,125, respectively. The total length of the river used for this analysis is 2150 m, and the average river width is 200 m. The river is separated into two flows at this region. On the boundary A–B, the velocity normal to the boundary $U_n = 1$ m/s is always imposed. On the boundaries A–F, E–D and B–C, the velocity normal to the boundary is assumed to be zero. Water elevation on the boundary A–B is specified as shown in Figure 14. Using the eddy viscosity $A_1 = 0{\cdot}4\,\mathrm{m}^2/\mathrm{s}$ and the friction coefficient $\lambda = 0{\cdot}008\,\mathrm{s}^{-1}$, the computation is performed based on the time increment $\Delta t = 0{\cdot}05$ s. Computed water elevation and velocity are represented in Figures (15)–(21) at steps 2000, 4000, 9600, 10,400, 20,800, 37,600 and 44,000. From this computation, the velocity and water elevation can be obtained according as the water elevation at the up-stream is rising up or falling down. It is also useful to decide how far the water is spread out in case of flood. To compute this example a CPU time of 150 min per 1000 steps was required on the FACOM M170F Computer.

CONCLUSION

The two-step explicit finite element method has been applied to the analysis of river flow. The procedures to solve the moving boundary problem have been presented and the stable computations have been obtained. Numerical illustration shows that the finite element method is entirely flexible for the analysis in which the complicated boundary configuration must be dealt with. Thus, the finite element method presented in this paper provides useful tools for the analysis of the design of river structures, improvement of flood plains and other engineering fields.

ACKNOWLEDGEMENTS

Computations presented in this paper have carried out with the help of Mr. T. Miwa, S. Mita, K. Nakamura and A. Anjyu, students of Chuo University, using the computers FACOM M170F of Chuo University and HITAC S810 of the University of Tokyo. A part of the research is supported by a Grant in Aid of Scientific Research, Ministry of Education, Government of Japan No. 60550330. The authors are grateful to the referee for suggestions and comments on this paper.

REFERENCES

1. J. F. Cochet, G. Dhatt, G. Hubert and G. Touzot, 'River and estuary flows by a new penalty finite element', in T. Kawai (ed.) *Finite Element Flow Analysis*, 1982, pp. 563–570.
2. T. Y. Su and S. Y. Wang, 'Depth-averaging models of river flow', in S. Y. Wang *et al.* (eds), *Finite Elements in Water Resources*, 1980, pp. 5.223–5.235.
3. J. K. Lee, 'Two-dimensional finite element analysis of the hydraulic effect of highway bridge fills in a complex flood plain', in S. Y. Wang *et al.* (eds), *Finite Elements in Water Resources*, 1980, pp. 6.3–6.23.
4. A. J. Baker and M. O. Soliman, 'On the accuracy and efficiency of a finite element algorithm for hydrodynamic flows', in K. P. Holz *et al.* (eds), *Finite Elements in Water Resources*, 1982, pp. 2.39–2.56.
5. M. Kawahara, H. Hirano, K. Tsubota and K. Inagaki, 'Selective lumping finite element method for shallow water flow', *Int. j. numer. methods fluids*, **2**, 89–112 (1982).
6. M. Kawahara and T. Yokoyama, 'Finite element method for direct runoff flow', *Proc. ASCE*, **106**, (HY4), 519–534 (1981).
7. M. Kawahara, M. Kobayashi and K. Nakata, 'A three-dimensional multiple level finite element method considering variable water density', in R. H. Gallagher *et al.* (eds), *Finite Elements in Fluids, Vol. 4*, Wiley, 1982, pp. 129–156.
8. M. Kawahara, M. Kobayashi and K. Nakata, 'Multiple level finite element analysis and its applications to tidal current flow in Tokyo Bay', *Appl. Math. Model*, **7**, 197–211 (1983).
9. M. Kawahara and K. Kashiyama, 'Selective lumping finite element method for nearshore current', *Int. j. numer. methods fluids*, **4**, 71–97 (1984).
10. M. Kawahara and T. Miwa, 'Finite element analysis of wave motion', *Int. j. numer. methods eng.*, **20**, 1193–1210 (1984).